Resolution of discrete excited states in $In_xGa_{1-x}N$ multiple quantum wells using degenerate four-wave mixing

D. O. Kundys,[1] J.-P. R. Wells,[1,*] A. D. Andreev,[2] S. A. Hashemizadeh,[1] T. Wang,[3] P. J. Parbrook,[3] A. M. Fox,[1] D. J. Mowbray,[1] and M. S. Skolnick[1]

[1]*Department of Physics and Astronomy, University of Sheffield, Sheffield S3 7RH, United Kingdom*

[2]*Advanced Technology Institute, University of Surrey, Guildford, GU2 7XH, United Kingdom*

[3]*EPSRC National Centre for III-V Technologies, University of Sheffield, Sheffield S1 3JD, United Kingdom*

(Received 15 August 2005; revised manuscript received 7 February 2006; published 11 April 2006)

We report on two pulse, degenerate four-wave mixing (DFWM) measurements on shallow $In_xGa_{1-x}N/GaN$ multiquantum wells (MQWs) grown on sapphire substrates. These reveal pulse length limited signal decays. We have found a 10:1 resonant enhancement of the DFWM signal at the excitonic transition frequencies which thereby give a sharp discrimination of the discrete excitonic contributions within the featureless distribution seen in absorption spectra. The exciton resonances have peak positions, which yield good overall agreement with a full $\mathbf{k}\cdot\mathbf{p}$ model calculation for the quantum well (QW) energy levels and optical transition matrix elements. $In_xGa_{1-x}N/GaN$ MQWs generally exhibit strongly inhomogeneously broadened excitation spectra due to indium fluctuation effects; this approach therefore affords a practical method to extract information on the excited excitonic states not available previously.

DOI: 10.1103/PhysRevB.73.165309 PACS number(s): 73.21.Fg, 78.47.+p, 78.55.Cr, 42.50.Md

I. INTRODUCTION

Wurtzite GaN-based alloys have attracted strong interest for optoelectronic applications, in particular the development of blue and UV light emitting diodes (LEDs) and laser diodes. The introduction of indium is significant due to the concomitant carrier localization and enhanced radiative quantum efficiency. However, the alloy nature leads to significant compositional disorder, which causes major broadening of the optical spectra. The lattice mismatch between InN and GaN also leads to strain induced spontaneous and piezoelectric polarization fields near the interface of a heterostructure and results in a quantum confined Stark effect (QCSE). This spatially separates the electron and hole in confined systems and reduces the optical transition strength.[1]

We report on two-pulse photon-echo experiments on low indium concentration, $In_xGa_{1-x}N$ multiquantum wells (MQWs) as a function of well thickness and excitation wavelength. Time-domain techniques have been extensively employed to study $In_xGa_{1-x}N$ structures, although for the most part these have concentrated on time-resolved photoluminescence studies.[2] Pump-probe techniques have also been used to study carrier relaxation and some of these studies have demonstrated quantum beats due to impulsive excitation of acoustic phonons.[3,4] Previous degenerate four-wave mixing (DFWM) spectroscopy in III-V nitrides has mostly concentrated on GaN epilayers where exciton dephasing times, exciton-exciton, exciton-impurity scattering, electron-phonon, and exciton-biexciton interactions have been studied.[5–8] Typically, dephasing times of ~1–2 ps are measured.

$In_xGa_{1-x}N$ epilayers and MQWs represent a highly inhomogeneously broadened system and excitonic resonances can be difficult to observe directly in a linear absorption spectrum. Our experiments reveal a pulse length limited, DFWM signal in both epilayers and MQWs. The measured signals are resonantly enhanced at the ground and excited states heavy-hole exciton absorption frequencies, yielding well-resolved resonances against the suppressed background of continuum states. From the dependence of the DFWM signal upon the intensity of the incident beams, it is concluded that the results may be strictly described in terms of the third-order optical susceptibility. We have used the resonant nature of these signals to determine the position of excited states in quantum wells of different thicknesses, yielding good agreement with model calculations.

II. EXPERIMENTAL DETAILS

The samples consisted of ten-period $In_{0.11}Ga_{0.89}N/GaN$ MQWs. In all cases, the barrier was 7.5 nm thick, and the quantum well thicknesses were varied between 1, 4, and 8 nm. All investigated samples were grown on (0001) sapphire double-polished substrates by metalorganic chemical vapor deposition (MOCVD). The substrates were initially treated in H_2 ambient at 1170 °C, followed by the growth of a 25 nm thick low-temperature (550 °C) GaN buffer layer and a 1.5 μm thick layer of nominally undoped GaN grown at a high temperature. Afterwards, the temperature was lowered to grow a ten-period MQW. The photoluminescent (PL) spectra were excited with a He–Cd laser, dispersed in a 0.75 m monochromator and detected with a GaAs photomultiplier tube. Photoluminescence excitation (PLE) spectra were obtained using a Xenon lamp with wavelength selectivity/tunability provided by a 0.25 m monochromator. Time-resolved spectroscopy was performed using a Ti-Sapphire oscillator yielding 150 fs pulses, tunable between 700 nm and 1 μm at a repetition rate of 80 MHz. To excite the interband transitions of $In_xGa_{1-x}N$ alloys, the oscillator output was frequency doubled, providing the required excitation wavelengths between 350 and 450 nm. The DFWM measurements were performed in a standard two-pulse, non-

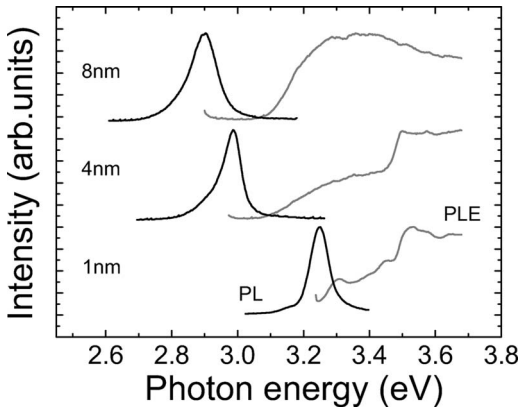

FIG. 1. 10 K PL and PLE of the $In_xGa_{1-x}N/GaN$ multiquantum well samples.

colinear "forward box," four-wave mixing geometry with the phase matched signal detected in the $|2\boldsymbol{k}_2-\boldsymbol{k}_1|$ direction, where $\boldsymbol{k}_1$ and $\boldsymbol{k}_2$ are the wave vectors of the echo-generating pulse sequence. The maximum available energy of the "dipole inverting" $\boldsymbol{k}_2$ pulse was 0.47 nJ with the $\boldsymbol{k}_1$ pulse held at an energy of 0.024 nJ. Both beams were focused using 5 cm focal length CaF_2 lenses onto the sample position, yielding a spot diameter of close to 50 μm. The signal was detected using a photomultiplier and a phase-sensitive detection scheme.

III. RESULTS AND ANALYSIS

Figure 1 shows the 10 K PL and PLE spectra of the three MQW samples. The PL spectrum for all samples shows a single-dominant peak at 3.25, 2.98, and 2.90 eV for the 1, 2, and 8 nm MQWs, respectively. By contrast, the PLE spectrum of the 1 nm thick sample shows one clear peak corresponding to the ground state *hh*1-*e*1 excitonic transition in the QW with some evidence for higher energy transitions. The PLE spectra for the 4 and 8 nm thick MQW samples reveal only a broad, structureless increase in absorption with no resolved features, which would be indicative of excitonic resonances. For the wider wells, a large shift of the PL from the onset of the quantum well interband absorption is observed. This shift results from a combination of the QCSE and exciton and carrier localization effects caused by indium disorder fluctuations.[9] It is significant that for the 4 nm and 8 nm thick MQWs samples, the PLE shows no absorption due to states close to the PL energy. This is due to a larger spatial separation of ground state electrons and holes in the wider wells and therefore weaker oscillator strengths of those transitions, which results in their suppression in PLE spectra. The featureless PLE spectra of the 4 and 8 nm MQWs arise due to the contribution of the excited states, which are significantly broadened due to their enhanced sensitivity to both well width *and* electric field fluctuations. This behavior is in contrast to GaAs quantum wells, which in the absence of electric fields display stronger broadening for narrow wells due to well width fluctuations.[10]

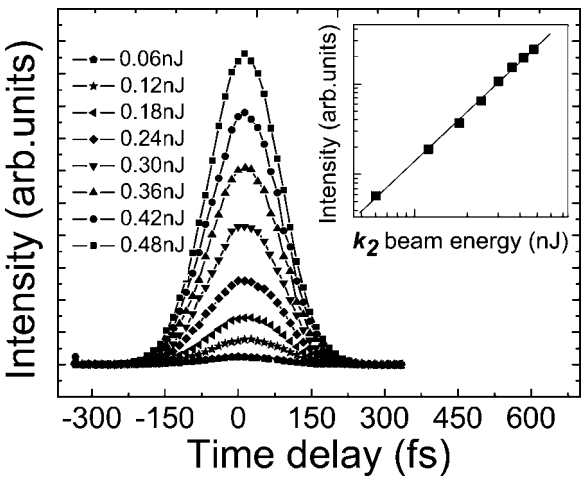

FIG. 2. Power dependence of the time-integrated DFWM signal in an 8 nm thick $In_xGa_{1-x}N/GaN$ MQW for a sample temperature of 5 K. The inset shows the logarithmic plot intensity dependence of the DFWM signal at zero delay (squares), and the linear fit (solid line); the line slope of 2 indicates the quadratic relation.

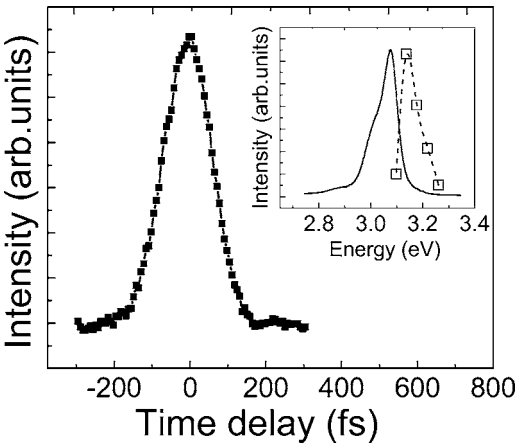

FIG. 3. DFWM signal for a 100 nm thick $In_{0.1}Ga_{0.9}N$ epilayer as measured at 5 K. The inset shows the normalized wavelength dependence of DFWM signal (open squares) fitted with a dashed line overlaid as a guide to the eye, and the PL (solid line) spectrum.

In our two-pulse DFWM experiments, the observed signal from all samples consists of a very fast, pulse length limited transient. In Fig. 2, the time-integrated (TI) DFWM signal is plotted as a function of the time delay between the generating pulses for the 8 nm thick sample. Transients are recorded for different energies of the $\boldsymbol{k}_2$ pulse with the $\boldsymbol{k}_1$ pulse energy kept constant at 0.024 nJ. The inset to Fig. 2 shows the intensity dependence of the DFWM signal at zero delay on a logarithmic scale; the data are fitted well with a line having a slope of 2, showing that we are within the $\chi^{(3)}$ limit. The very fast dephasing we observe is an order of magnitude faster than that observed in GaN epilayers.[5–8] The fast dephasing times observed are most likely attributable to the alloy disorder, which leads to a disorder induced dephasing[11] that is dependent on high indium concentrations. An additional contributing factor may be carrier escape tunneling,[12] which can take place due to the built-in electric field in $In_xGa_{1-x}N/GaN$ MQWs.

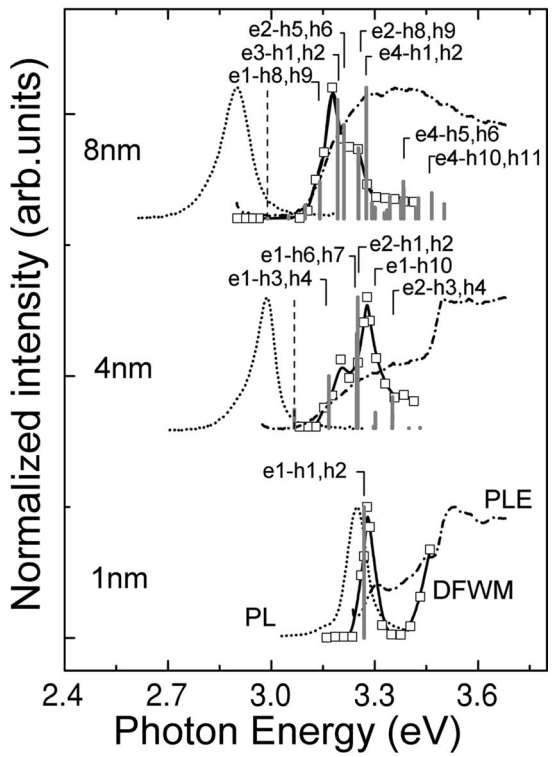

FIG. 4. The wavelength dependence of the normalized DFWM signal (open squares) overlaid on the PL and PLE spectra for the 1, 4, and 8 nm MQWs. The vertical gray lines represent the spectral position (and transition energy) of the interband transitions, which have a high oscillator strength. The height of the gray lines is proportional to the absorption strength. The black vertical dashed lines represent *only* the spectral position of the ground state transition in the model calculation (the transition intensities are negligible).

We have also performed a study of a 100 nm thick $In_{0.1}Ga_{0.9}N$ epilayer. We found a pulse limited time-integrated DFWM signal that is enhanced at the epilayer band-edge energy (see Fig. 3). The wavelength dependence of the DFWM signal observed in the epilayer shows a single peak whose intensity increases rapidly from the low-energy side, with a shoulder on the high-energy side reflecting the span of the free-exciton splitting influenced by the band gap bowing in $In_xGa_{1-x}N$. This result indicates that DFWM in $In_xGa_{1-x}N$ systems is enhanced at the excitonic states of the system, a result we show is fully borne out by the measurements on the QWs.

Figure 4 shows DFWM signals measured at different excitation wavelengths (for the three QW samples discussed above) with a fixed excitation density of 6.4 $\mu J/cm^2$. These are plotted together with the normalized PL and PLE spectra for each of the samples. Surprisingly, given the broad featureless nature of the PLE for these samples, the DFWM results show clear resonances at specific wavelengths. Concentrating on the results for the 1 nm thick sample to begin with, it is immediately evident that the nonlinear signal is resonantly enhanced at the lowest $e1$-$hh1$ transition of the quantum well. Hence we conclude that the enhancement of the DFWM signal at a specific wavelength indicates the position of the excitonic energy levels in the QW. The DFWM signal is also observed to increase just below the barrier energy, which may arise either from a shoulder of strong DFWM signal from the GaN epilayer, or from the presence of a QW state nearly resonant with the barrier band edge in the PLE spectrum.

For the wider wells, the DFWM spectra are more complex with a number of overlapping transitions observed. Such rich structure is suggestive of the observation of excited state transitions within the wells. There is no signal detected for wavelengths close to the PL peak wavelengths in both the 4 and 8 nm thick samples. This is due to the pronounced quantum confined Stark effect (QCSE) in the wider wells, leading to weak wave-function overlap for the $e1$-$hh1$ transition. The key observation is that clear and distinct resonances can be

TABLE I. Material band structure parameters

Parameter	GaN	InN	$In_{0.11}Ga_{0.89}N$
Lattice constants			
c (nm)	0.5185	0.5703	0.5242
a (nm)	0.3189	0.3545	0.3228
Valence band effective mass parameters			
A_1	−7.21	−8.21	−7.32
A_2	−0.44	−0.68	−0.47
A_3	6.68	7.57	6.78
A_4	−3.46	−5.23	−3.65
A_5	−3.40	−5.11	−3.59
A_6	−4.90	−5.96	−5.02
Deformation potentials[a]			
a_c (eV)	−4.08		−4.08
D_1	0.7		0.7
D_2	2.1		2.1
D_3	1.4		1.4
D_4	−0.7		−0.7
Energy parameters			
Δ_1 ($=\Delta_{cr}$) (eV)	0.010	0.040	0.013
$\Delta_2=\Delta_3=\Delta_{so}/3$ (eV)	0.005	0.0016	0.0046
$E_g^{(10\ K)}$ (eV)	3.51	0.78	3.07
			b (eV)=1.4
Conduction band effective masses			
m_e^z (m_0)	0.20	0.14	0.19
m_e^t (m_0)	0.18	0.1	0.17
Dielectric constant			
ε	10.28	14.61	10.756
Elastic stiffness constants			
C_{11} (GPa)	390	223	371.6
C_{12} (GPa)	145	115	141.7
C_{13} (GPa)	106	92	104.5
C_{33} (GPa)	398	224	378.9
PZ constants			
d_{31} (pm/V)	−.6	−3.5	−1.81
d_{33} (pm/V)	3.1	7.6	3.59

[a]Reference 13.

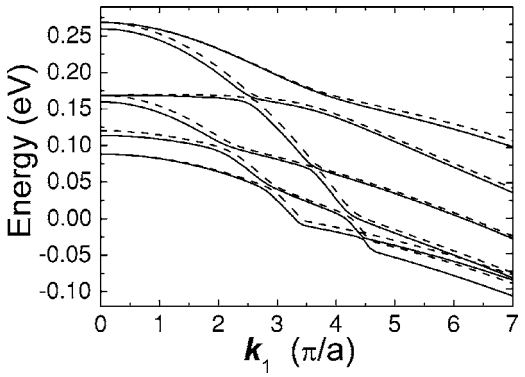

FIG. 5. The in-plane dispersion of the valence subbands along $\langle 100 \rangle$ direction for 4 nm MQW sample (a=4 nm). The calculation results obtained using the 8×8 and 4×4 models are indicated with solid and dashed lines, respectively.

observed in DFWM even though none are present in the PLE spectra with the exception of the 1 nm sample where the $e1$-$hh1$ transition has large oscillator strength.

In order to exemplify that the DFWM signal is shaped by transitions with strong oscillator strength, we employed a multiband $\mathbf{k}\cdot\mathbf{p}$ model for the wurtzite semiconductor to calculate the energy levels and optical transition matrix elements for the samples studied. The $\mathbf{k}\cdot\mathbf{p}$ Hamiltonian employed, including strain and band mixing effects, is described in detail in Refs. 13 and 14. To calculate the energy levels and optical matrix elements, we used the plane-wave expansion method.[14,15] We used both 8×8 and 4×4 models; the 4×4 model is obtained from the 8×8 model by taking the spin-orbit splitting $\Delta_3=0$. Since for InN and GaN this splitting is very small (Δ_3=4.6 meV, see Table I), in Fig. 5 one can see that both models give very similar results (in the 8×8 model we obtain a small additional splitting of the order of Δ_3 for some of the transitions; for the purposes of the present paper this splitting is not important), so we present here the results obtained from the 4×4 model. Recently, we have shown that the uncertainty in both the elastic and piezoelectric constants leads to a significant inaccuracy in calculated transition energies.[16] The electric field was taken as an adjustable parameter in order to fit the QW ground state transition to our PL data with a reassuring "Stokes" shift of less than 80 meV. The values employed in our calculations of 1.2, 1, and 0.45 MV/cm for the 1, 4, and 8 nm MQWs, respectively, are consistent with the findings of Ref. 17, where a reduction of the electric field was found with increasing well width. Table I shows the numerical values of the material constants used in the $\mathbf{k}\cdot\mathbf{p}$ band calculations for unstrained materials, and are taken from Ref. 18, unless otherwise indicated. The alloy properties of $In_xGa_{1-x}N$ are obtained by linear interpolation except for the energy gap, where the relation from Ref. 19 is used.

In Fig. 4, the vertical gray lines indicate the results of the calculation with the line height representing absorption strengths of the relative interband transitions for each of the samples, while their spectral position represents the transition energy. The calculation of the 1 nm QW transition energies shows the presence of only the ground state exciton transition at an energy of 3269 meV, while a more complex structure is observed for the 4 and 8 nm QWs. As we can see from Fig. 4, the simulation gives good agreement for all studied QW samples, proving that the peaks in the DFWM trend indicate the position of high oscillator strength transitions (see Table II for details). In the 1 nm QW sample the peak in the DFWM signal corresponds to the ground state $e1$-$hh1$ transition and yields a single intense resonance. For the 4 nm QW sample, the calculated transitions are redshifted by approximately 35 meV from the experimental DFWM signal peaks; however, the general trend is similar and the relative intensities approximately correct. For the 8 nm thick sample, the situation is more complex due to the multitude of possible transitions (Fig. 4). It is clear that for both the 4 and 8 nm MQWs the DFWM spectra are determined by excited state transitions, the ground state transitions being unobservable due to their very weak oscillator strengths. Good overall agreement is obtained and the calcu-

TABLE II. Calculated absorption strength at $k_x=0$ and their transition energies for 1, 4, and 8 nm $In_xGa_{1-x}N$ QW used in Fig. 4. The spin-orbit splitting of $\sim$10 meV is neglected in order to simplify the presentation of calculation results.

	Transition label	Normalized absorption strength (a.u.)	Transition energy (eV)
1 nm QW	$e1$-$h1$, $h2$	1, 0.41	3.269
4 nm QW	$e1$-$h1$, $h2$	0.05, 0.14	3.067
	$e1$-$h3$, $h4$	0.31, 0.21	3.167
	$e1$-$h6$, $h7$	0.44, 0.52	3.247
	$e2$-$h1$, $h2$	0.33, 1	3.251
	$e1$-$h10$	0.16	3.301
	$e2$-$h3$, $h4$	0.18, 0.14	3.351
8 nm QW	$e1$-$h1$, $h2$	0, 0	2.989
	$e1$-$h5$, $h6$	0.06, 0.06	3.097
	$e1$-$h8$, $h9$	0.13, 0.23	3.140
	$e1$-$h10$, $h11$	0.37, 0.35	3.180
	$e1$-$h12$, $h13$	0.49, 0.48	3.216
	$e2$-$h1$, $h2$	0.04, 0.14	3.102
	$e2$-$h3$, $h4$	0.29, 0.24	3.162
	$e2$-$h5$, $h6$	0.47, 0.45	3.210
	$e2$-$h8$, $h9$	0.23, 0.44	3.253
	$e2$-$h10$, $h11$	0.07, 0.07	3.292
	$e3$-$h1$, $h2$	0.25, 0.89	3.193
	$e3$-$h8$, $h9$	0.07, 0.15	3.252
	$e3$-$h10$, $h11$	0.17, 0.18	3.383
	$e4$-$h1$, $h2$	0.26, 1	3.275
	$e4$-$h5$, $h6$	0.14, 0.15	3.384
	$e4$-$h8$, $h9$	0.07, 0.14	3.427
	$e4$-$h10$, $h11$	0.12, 0.13	3.466
	$e4$-$h12$, $h13$	0.06, 0.08	3.502
	$e5$-$h3$, $h4$	0.1, 0.09	3.375

lations indicate that the resonances observed in the DFWM experiments reflect excitonic transitions within the quantum well. The MQWs systems we have investigated have a complex valence band structure,[2,20,21] which are nonisotropic, nonparabolic, and semidegenerate. Thus for the wider wells it is impractical to label all of the transitions. The essential points to be made are: (i) the DFWM spectra indicate the position of excited states in the quantum wells, (ii) the spectra are shaped by strong oscillator strength transitions even though the precise assignments cannot be considered definitive, and (iii) the wider wells do not show transitions from low-lying quantum well states due to the low oscillator strength of transitions arising from those levels.

Early studies on GaAs QWs (Refs. 22 and 23) revealed that DFWM signals in quantum wells are generally dominated by excitonic contributions and that this is primarily due to the large ratio of the exciton to free-carrier dephasing rates. These early reports concluded that DFWM experiments performed with short pulses ($\sim$100 fs) always measure signals due to excitons even when more free carriers than excitons are created, since the longest dephasing time always dominates. This is the case even if the exciton is only weakly excited by the tail of the pulse. The presence of a large number of potential scattering states facilitates fast dephasing of the continuum states in GaAs QWs and this yields bigger contrast in the relative dephasing rates. In fact, in Ref. 22, a 300:1 excitonic resonance was observed. In our case the DFWM experiment picks out localized states with a longer dephasing time from "less localized" states. Thus, contrary to GaAs, $In_xGa_{1-x}N$ MQWs DFWM signals represent the selective excitation of more heavily localized states from the distribution that is available, and discriminates against the broad background of "continuum" states with shorter dephasing times.

IV. CONCLUSIONS

To summarize, we have performed two-pulse DFWM experiments on $In_xGa_{1-x}N/GaN$ MQWs which reveal pulse length limited, transient signals. We have observed a resonant enhancement of the DFWM signal at specific wavelengths. Calculations confirm that these signals correspond to excitonic transitions within the quantum wells. The spectral dependence of DFWM provides an alternate way to investigate excited state levels in nitride quantum wells with discrimination against the free-carrier continuum, information that cannot be obtained using PLE from the highly inhomogeneous $In_xGa_{1-x}N$ MQWs.

ACKNOWLEDGMENTS

This work has been supported by the EPSRC through Grant Nos. GR/S24251/01 and GR/R84955/01.

*Corresponding author. Email address: j.p.wells@sheffield.ac.uk

[1] B. Gil, *Low Dimensional Nitride Semiconductors* (Oxford University Press, New York, 2002).
[2] E. Berkowicz, D. Gershoni, G. Bahir, E. Lakin, D. Shilo, E. Zolotoyabko, A. C. Abare, S. P. Denbaars, and L. A. Coldren, Phys. Rev. B **61**, 10994 (2000).
[3] C.-K. Sun, J.-C. Liang, and X.-Y. Yu, Phys. Rev. Lett. **84**, 179 (2000).
[4] Ü. Özgür, C.-W. Lee, and H. O. Everitt, Phys. Rev. Lett. **86**, 5604 (2001).
[5] A. J. Fischer, W. Shan, G. H. Park, J. J. Song, D. S. Kim, D. S. Yee, R. Horning, and B. Goldenberg, Phys. Rev. B **56**, 1077 (1997).
[6] S. Pau, J. Kuhl, F. Scholz, V. Haerle, M. A. Khan, and C. J. Sun, Phys. Rev. B **56**, R12718 (1997).
[7] S. Pau, J. Kuhl, F. Scholz, V. Haerle, M. A. Khan, and C. J. Sun, Appl. Phys. Lett. **72**, 557 (1998).
[8] K. Kyhm, R. A. Taylor, J. F. Ryan, T. Aoki, M. Kuwata-Gonokami, B. Beaumont, and P. Gibart, Phys. Rev. B **65**, 193102 (2002).
[9] P. Lefebvre, A. Morel, M. Gallart, T. Taliercio, J. Allégre, B. Gil, H. Mathieu, B. Damilano, N. Grandjean, and J. Massies, Appl. Phys. Lett. **78**, 1252 (2001).
[10] W. Langbein, P. Borri, and J. M. Hvam, Mater. Sci. Forum **297-298**, 73 (1999).
[11] Ch. Lonsky, P. Thomas, and A. Weller, Phys. Rev. Lett. **63**, 652 (1989).
[12] G. von Plessen, J. Feldmann, K. W. Goossen, B. Schlichtherle, E. O. Göbel, D. A. B. Miller, and J. E. Cunningham, Semicond. Sci. Technol. **9**, 523 (1994).
[13] S. L. Chuang and C. S. Chang, Phys. Rev. B **54**, 2491 (1996).
[14] A. D. Andreev and E. P. O'Reilly, Phys. Rev. B **62**, 15851 (2000).
[15] A. D. Andreev and R. A. Suris, Semiconductors **30**(3), 285 (1996).
[16] Ursula M. E. Christmas, A. D. Andreev, and D. A. Faux, J. Appl. Phys. **98**, 073522 (2005).
[17] M. Stevens, A. Bell, M. R. McCartney, F. A. Ponce, H. Marui, and S. Tanaka, Appl. Phys. Lett. **85**, 4651 (2004).
[18] I. Vurgaftman and J. R. Meyer, J. Appl. Phys. **94**, 3675 (2003).
[19] K. Osamura, S. Naka, and Y. Murakami, J. Appl. Phys. **46**, 4342 (1975).
[20] Joachim Piprek, R. Kehi Sink, Monica A. Hansen, John E. Bowers, and Steve P. DenBaars, in *Physics and Simulation of Optoelectronic Devices VIII*, edited by R. Binder, P. Blood, and M. Osinski (International Society for Optical Engineering, Bellingham, WA, 2000).
[21] Y. C. Yeo, T. C. Chong, M. F. Li, and W. J. Fan, J. Appl. Phys. **84**, 1813 (1998).
[22] D. S. Kim, J. Shah, J. E. Cunningham, T. C. Damen, W. Schäfer, M. Hartmann, and S. Schmitt-Rink, Phys. Rev. Lett. **68**, 1006 (1992).
[23] J. Shah, *Ultrafast Spectroscopy of Semiconductors and Semiconductor Nanostructures* (Springer-Verlag, Berlin, 1999).